Memory Decoding Algorithm for FSO Transmission

1st Yu-Jung Chu
Electrical and Computer Engineering
Oregon State University
Corvallis, Oregon 97331–5501
chuy@oregonstate.edu

2nd Thinh Nguyen
Electrical and Computer Engineering
Oregon State University
Corvallis, Oregon 97331–5501
thinhq@eecs.oregonstate.edu

Abstract—Due to the limitation of the radio frequency (RF) spectrum, it is increasingly more difficult to support billions of wireless devices in the age of Internet-of-Things. Consequently, many recent wireless indoor communication systems have been developed using free space optical (FSO) communication technologies that exploit the extremely large light spectrum to transmit data. However, FSO technologies, especially when using On-Off Keying(OOK) modulation, the Light-Emitting-Diode (LED) transmitters produce an inherent non-linear distortion in the output. Effectively, the LED acts as a band-limited channel between the inputs and outputs. In this paper, we utilize a mathematical model to capture the distortion of the output for a given input. Based on the mathematical model, we developed a technique called Memory Decoding Algorithm (MDA) used at a receiver and effectively reduces the bit error rates via maximum likelihood decoding principle when On-Off Keying(OOK) modulation is used. Both theoretical analyses and simulation results show that the proposed technique outperforms the conventional methods such as linear equalization.

Index Terms—Memory Decoding, MDA, WiFO, FSO, Free Space Optical, PAM, OOK

I. Introduction and Related Work

Due to the limitation of the radio frequency (RF) spectrum, it is increasingly more difficult to support billions of wireless devices in the age of Internet-of-Things. Consequently, recent researches on RF-based communications have focused on expanding and using RF spectrum more efficiently. There have been numerous techniques to increase spectrum efficiency, ranging from physical layer techniques such as Multiple Input Multiple Output (MIMO) transmissions to higher level approaches such as Dynamic Spectrum Access (DSA). However, due to many economic and technical issues, the proliferation of DSA remains to be seen. Free space optical (FSO) communication technologies promise a complementary approach to the spectrum scarcity problem. Although, the visible light spectrum is extremely large, ranging from hundreds of Gigahertz to Petahertz, as compared to the RF/Microwave spectrum that occupies a relatively much smaller band (a few Kilohertz to hundreds of Gigahertz). However, the main factors that limit the capacities of FSO communication systems are technologies. FSO communication transmits information by modulating light. As such, the transmission rate depends on how fast a transmitter can modulate light and how fast a receiver can reliably decode a light signal. Recently, solid state light sources such as Light Emitting Diodes (LEDs) and laser diodes are sufficiently mature enough so that it is practical to transmit high data rates at reliably short ranges. LEDs also have advantages such as low power consumption and low costs, as such they are widely studied in FSO communities [1] - [5]. However, [1] - [4] are studies working on outdoor and long-distance implementations of hybrid FSO/RF communication systems. These hybrid systems were affected by attenuation and fading due to distances, weather conditions and scintillation. Little research effort has been put into indoor free-space optical communications as [5]. In practice, LED transmitters have maximum modulation frequency before the output signals become too distorted. There is also an inherent trade-off between the output power (light intensity) and the modulation frequency. As for the receiving side, a photo-diode is used to turn light intensity into current/voltage, i.e., decoding. Thus, FSO communication systems are designed with the appropriate transmitters, receivers, and usage scenarios to maximize the transmission rate.

In communication, the popular method for compensating the distortion is to use linear equalization to cancel the effect of distortion by the channel. For example, many adaptive MMSE equalizer schemes were proposed to suppress the multipath ISI (inter symbol interference) in [6]. [7] presents an effective analogue equalization to enhance the modulation bandwidth of an organic light emitting diode (OLED). However, linear equalization techniques are typically used for high-order modulation, e.g. PAM-16, where accurate decoding of different signal levels is crucial. When On-Off Keying modulation is used, linear equalization techniques offer minimal advantages while incurring other costs such as increasing power consumption and lower speed which are due the requirement of an accurate Analog-to-Digital Converter(ADC). We also note that since the shapes of different distorted transmitted signals are known, a matched filter [8] [9] can be used at the receiver to detect the most probable transmitted signal to reduce the bit error rate. However, digital matched filters require a high precision ADC converter and more digital processing power to accurately match the shape. On the other hand, the proposed MDA technique only requires 1 or 2 samples per symbol. There is also

analog implementation of matched filter, but the analog implementation is not sufficiently flexible (programmable) for our WiFO system. Both Partial Response Maximum Likelihood(PRML) [10] [11] and Maximum Likelihood Sequence Estimation (MLSE) employ coded schemes to improve the bit error rate at the expense of lower throughput. However, MDA does not use coding thus has less overhead. Unlike many other techniques, our proposed MDA exploits the specific non-linear and memory LED-response during the decoding. This leads to lower bit error rate than a typical generic linear equalization technique as shown in Section IV. Furthermore, the proposed MDA does not require an ADC which leads to power efficient and fast circuit implementation.

This paper is focused on how to transmit information fast and reliably using On-Off Keying modulation under the distortion caused by an LED-based transmitter. In particular, the LED acts as a band-limited channel between the inputs and outputs. As a result, high-frequency components of the input signal are attenuated, resulting in the distorted output, i.e., when the data rate is high, the output will be more distorted. Consequently, without any correction for the distortion, the bit error rate will be higher. To reduce the bit error rates, we proposed a memory based decoding algorithm called MDA, which utilizes 1) a mathematical model to estimate the distortion of the light output for a given input when On-Off Keying is used and 2) maximum likelihood principle to derive the dynamic decoding thresholds to reduce the bit error rate. The outline of the paper is as follows. First we will describe the mathematical model for the LED distortion in Section II. Then Section III and IV are devoted to the analysis and performance of the proposed MDA technique. Finally we conclude with a few remarks in Section V.

II. LED Response Model

The overall impulse response of an LED-based communication system depends on multiple factors. These include the characteristics of the LED at the transmitter, the photo-diode used at the receiver, the driver circuits associated with the transmitter and receiver, and propagation medium. In our application scenario, particularly the WiFO system [12], which we have been developing over several years, uses short and focused FSO transmissions. As a result, multi-path fading due to light propagation is negligible. The primary signal distortion come from the LED, photo-diode, their driver circuits, and the attenuation due to the distance between the transmitter and the receiver. Therefore, although the impulse response of a considered FSO channel is device dependent, and can be empirically measured and calibrated, using LTI techniques such as inverting the impulse response in the frequency domain is difficult to implement.

Fig. 1 shows the measured response at the receiver photo-diode when a pulse train is sent at $1.\overline{66}$ MHz. This follows the fact that the LED output pulse has

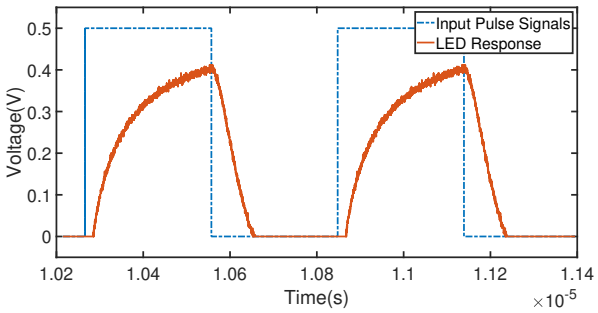

Fig. 1: LED Pulse Response

an exponential rise and fall portions, as well as a little delay before the LED's full turn-on and turn-off. From physics, the characteristic time constant for the rise and fall portions of the pulse are related to the photon's net recombination time τ. Ideally, the rise time τ_R, (the time for the voltage to go from 10% to 90% of the maximum voltage of the light output), and the fall time τ_F (the time for the voltage to go from 90% to 10% of the maximum voltage), are the same and equal to 2.2τ [13]. In practice, the net recombination time τ itself depends on the circuit implementation to drive the LEDs and photo-diode. Thus, different values for τ_R and τ_F are often observed in real-world settings. Based on this, we use τ_a and τ_b for charging and discharging respectively to replace the photon's net recombination time, τ. Eq.(1) and Eq.(2) approximate the LED voltage responses while the sending bit is "1" and "0" respectively. V_{max} in Eq.(1) and Eq.(2) is the maximum response voltage of the LED, this value can be empirically measured at the receiver by sending multiple consecutive "1"s. By analyzing the measured data of the LED response, we can numerically obtain the parameters τ_a and τ_b. Eq.(1) is also the impulse response for an RC circuit, however, due to the different values observed for τ_a and τ_b, inverting Eq.(1) to cancel the channel is impractical. Fig. 2 shows the measured LED responses of a high speed infrared emitting diodes(850nm, VSMY2850) and the mathematically modeled response for the cases of 1M Hz and 25M Hz input pulse trains.

$$V_{response_1}(t) = V_{max} \cdot (1 - e^{-\frac{t}{\tau_a}}) \tag{1}$$

$$V_{response_0}(t) = V_{max} \cdot e^{-\frac{t}{\tau_b}} \tag{2}$$

III. Memory Decoding

In this section, we describe a post-distortion algorithm called Memory Decoding Algorithm (MDA) used by the receiver to reduce the bit error rate. Using this technique, there is no need for the transmitter to pre-distort the signal. Instead, based on the mathematical model of the channel response in Eqs. (1) and (2), MDA uses the maximum likelihood method for decoding the bits.

Using the OOK modulation, the transmitted signal $x(t)$ can be considered as a telegraph pulse train that has only

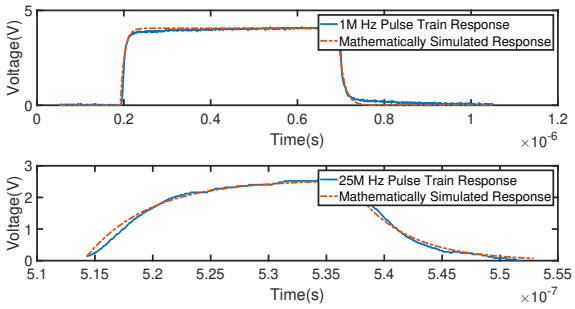

Fig. 2: LED Pulse Response vs. Simulated Response for 1 MHz and 25 MHz

two distinct values, 0 and 1. We note that for a given LED transmitter, the effective channel can be modelled as a band-limited channel. Thus, a transmitted signal whose significant amount of energy is in the high frequency band (outside the channel bandwidth) will be distorted greatly. In this section, we assume that the rate of transmitted signal is within the bandwidth of the LED. In the time domain, it is equivalent to assuming that the sending rate is sufficiently low such that it only takes at most one sending duration, T, for the voltage to reach V_{max} from 0. Similarly, it also takes at most one sending duration, T, for the voltage to go from V_{max} down to 0. We now propose a threshold decoding method using the previous decoded results as well as the adaptive thresholds to decode the current bit.

A. Decoding Algorithm

We model the received signal as:

$$\tilde{y}(t) = y(t) + N(t), \tag{3}$$

where $N(t)$ is a white noise.

At receiver, $\tilde{y}(t)$ is sampled at $(i-1)T + T_s$ for the i^{th} bit. The classical threshold decoding scheme decodes

$$\tilde{y}((i-1)T+T_s) = \begin{cases} 1 & \text{if } \tilde{y}((i-1)T+T_s) \geq \frac{V_{max}}{2}, \\ 0 & \text{otherwise.} \end{cases}$$

It can be shown that using a fixed threshold of $\frac{V_{max}}{2}$, is suboptimal. Therefore, we propose a novel decoding scheme that utilizes the "memory" property of LED response.

Assuming that the memory only lasts for one bit duration, T, i.e., $e^{-\frac{t}{\tau_a}} \cong 0$ and $e^{-\frac{t}{\tau_b}} \cong 0$ when $t \geq T$, the observed i^{th} received sample is simplified to

$$\tilde{y}_i = \begin{cases} 0 + N_i, & if\ x_{i-1} = 0\ and\ x_i = 0 \\ V_{max} \cdot e^{-\frac{T_s}{\tau_b}} + N_i, & if\ x_{i-1} = 1\ and\ x_i = 0 \\ V_{max} \cdot (1 - e^{-\frac{T_s}{\tau_a}}) + N_i, & if\ x_{i-1} = 0\ and\ x_i = 1 \\ V_{max} + N_i, & if\ x_{i-1} = 1\ and\ x_i = 1 \end{cases}, \tag{4}$$

where x_i denotes the i^{th} transmitted bit and N_i is a random variable representing the channel noise, which is independent of x_i and its response. Thus, each current bit depends on both the current and the previous bits. Applying the MLE (Maximum Likelihood Estimation) analysis, the decoding rule of current bit can be found as:

$$\hat{x}_i = \begin{cases} 1 & \text{if } \frac{f_{N_i}(\tilde{y}_i - y_i \mid x_{i-1}, x_i = 1, \tilde{y}_i)}{f_{N_i}(\tilde{y}_i - y_i \mid x_{i-1}, x_i = 0, \tilde{y}_i)} \geq 1 \\ 0 & \text{otherwise} \end{cases}, \tag{5}$$

where $f_{N_i}(\cdot)$ represents the probability density function of the noise, N_i.

It is important to note that the proposed algorithm makes use of x_{i-1}, the correct transmitted bit in the previous time slot. However, x_{i-1} is not available at the receiver. To that end, we make the assumption that the decoded bit in the previous time slot, $\hat{x}_{i-1}$, is the same as the true transmitted bit, x_{i-1}. Consequently, our algorithm uses $\hat{x}_{i-1}$ in place of x_{i-1} in Eq.(5). Although this approximation might introduce error propagation during decoding, our theoretical analysis and simulation will show that the error propagation is minimal.

The decoding algorithm based on Eq.(5) can be simplified to an adaptive threshold decoding algorithm involving two optimal thresholds TH_0 and TH_1. This is in contrast with the classical thresholding decoding algorithm where only one threshold is used. As an example, we derive the optimal thresholds TH_0 and TH_1 assuming an additive white Gaussian noise (AWGN) as follows.

Plugging $x_{i-1} = \hat{x}_{i-1} = 0$ and Eq.(4) in the inequality (5), we obtain

$$\begin{aligned} &\frac{f_{N_i}(\tilde{y}_i - y_i \mid x_{i-1} = 0, x_i = 1, \tilde{y}_i)}{f_{N_i}(\tilde{y}_i - y_i \mid x_{i-1} = 0, x_i = 0, \tilde{y}_i)} \geq 1 \\ \Rightarrow\ &\frac{f_{N_i}(\tilde{y}_i - V_{max}(1 - e^{-\frac{T_s}{\tau_a}}))}{f_{N_i}(\tilde{y}_i - 0)} \geq 1 \\ \Rightarrow\ &\tilde{y}_i \geq \frac{V_{max}(1 - e^{-\frac{T_s}{\tau_a}})}{2} = TH_0. \end{aligned} \tag{6}$$

Applying the same rule and plugging $x_{i-1} = \hat{x}_{i-1} = 1$ and Equation (4) in the inequality (5), we obtain

$$\begin{aligned} &\frac{f_{N_i}(\tilde{y}_i - y_i \mid x_{i-1} = 1, x_i = 1, \tilde{y}_i)}{f_{N_i}(\tilde{y}_i - y_i \mid x_{i-1} = 1, x_i = 0, \tilde{y}_i)} \geq 1 \\ \Rightarrow\ &\frac{f_{N_i}(\tilde{y}_i - V_{max})}{f_{N_i}(\tilde{y}_i - V_{max} e^{-\frac{T_s}{\tau_b}})} \geq 1 \\ \Rightarrow\ &\tilde{y}_i \geq \frac{V_{max}(1 + e^{-\frac{T_s}{\tau_b}})}{2} = TH_1. \end{aligned} \tag{7}$$

Using the optimal TH_0 and TH_1, the MDA for decoding a block of N bits is summarized in Algorithm 1.

B. Bit Error Rate Analysis

In this section, we provide analysis for bit error rate of the proposed MDA using a Finite Markov Chain. First, we define the states, S_k, $k = 0, 1, \cdots, 7$, for a discrete-time stochastic process, X_n, $n = 0, 1, 2, \cdots$, in the Markov Chain, where S_k represents a tuple consisting of previously decoded bit, previously sent bit, and current transmitted

Algorithm 1 Memory Decoding Algorithm

Require: Initial parameters : TH_0, TH_1, N, $\hat{x}_0 = 0$

```
for i = 1 to N do
    if x̂_{i-1} == 0 then
        Threshold = TH_0
    else                                   ▷ x̂_{i-1} == 1
        Threshold = TH_1
    end if
    if ỹ_i ≥ Threshold then
        x̂_i = 1;
    else
        x̂_i = 0;
    end if
end for
```

bit, i.e., $(\hat{x}_{i-1}, x_{i-1}, x_i)$. We order the states S_k as follows: S_0 is defined as $(0,0,0)$, S_1 is defined as $(1,0,0)$, S_2 is defined as $(0,1,0)$, $\cdots$, and S_7 is defined as $(1,1,1)$. To construct the transition matrix P for the Markov chain, we compute the transition probabilities, $P\{X_n \mid X_{n-1}\}$. For example, let us compute $P\{X_n = S_1 \mid X_{n-1} = S_0\}$. Using the optimal TH_0 and TH_1 we derived previously and Eq.(4), we have:

$$\begin{aligned} &P\{X_n = S_1 \mid X_{n-1} = S_0\} \\ &= \frac{1}{2} \cdot P(\tilde{y}_i \geq TH_0 \mid \hat{x}_{i-1} = 0,\ x_{i-1} = 0,\ x_i = 0) \\ &= \frac{1}{2} \cdot P(N_i \geq TH_0) = \frac{1}{2} \cdot \{1 - F_{N_i}(TH_0)\}, \end{aligned} \tag{8}$$

where $F_{N_i}(\cdot)$ denotes the cumulative distribution function of the random variable, N_i. The transition matrix P is then obtained as

$$P = \begin{bmatrix} \frac{1}{2}F_{N_i}(TH_0) & \frac{1}{2}\{1-F_{N_i}(TH_0)\} & 0 & 0 & \frac{1}{2}F_{N_i}(TH_0) & \frac{1}{2}\{1-F_{N_i}(TH_0)\} & 0 & 0 \\ \frac{1}{2}F_{N_i}(TH_1) & \frac{1}{2}\{1-F_{N_i}(TH_1)\} & 0 & 0 & \frac{1}{2}F_{N_i}(TH_1) & \frac{1}{2}\{1-F_{N_i}(TH_1)\} & 0 & 0 \\ \frac{1}{2}F_{N_i}(l) & \frac{1}{2}\{1-F_{N_i}(l)\} & 0 & 0 & \frac{1}{2}F_{N_i}(l) & \frac{1}{2}\{1-F_{N_i}(l)\} & 0 & 0 \\ \frac{1}{2}F_{N_i}(m) & \frac{1}{2}\{1-F_{N_i}(m)\} & 0 & 0 & \frac{1}{2}F_{N_i}(m) & \frac{1}{2}\{1-F_{N_i}(m)\} & 0 & 0 \\ 0 & 0 & \frac{1}{2}F_{N_i}(s) & \frac{1}{2}\{1-F_{N_i}(s)\} & 0 & 0 & \frac{1}{2}F_{N_i}(s) & \frac{1}{2}\{1-F_{N_i}(s)\} \\ 0 & 0 & \frac{1}{2}F_{N_i}(u) & \frac{1}{2}\{1-F_{N_i}(u)\} & 0 & 0 & \frac{1}{2}F_{N_i}(u) & \frac{1}{2}\{1-F_{N_i}(u)\} \\ 0 & 0 & \frac{1}{2}F_{N_i}(q) & \frac{1}{2}\{1-F_{N_i}(q)\} & 0 & 0 & \frac{1}{2}F_{N_i}(q) & \frac{1}{2}\{1-F_{N_i}(q)\} \\ 0 & 0 & \frac{1}{2}F_{N_i}(r) & \frac{1}{2}\{1-F_{N_i}(r)\} & 0 & 0 & \frac{1}{2}F_{N_i}(r) & \frac{1}{2}\{1-F_{N_i}(r)\} \end{bmatrix}, \tag{9}$$

where

$$\begin{aligned} l &= TH_0 - V_{max}e^{-\frac{T_s}{\tau_b}} & m &= TH_1 - V_{max}e^{-\frac{T_s}{\tau_b}} \\ s &= TH_0 - V_{max}(1-e^{-\frac{T_s}{\tau_a}}) & u &= TH_1 - V_{max}(1-e^{-\frac{T_s}{\tau_a}}) \\ q &= TH_0 - V_{max} & r &= TH_1 - V_{max}. \end{aligned} \tag{10}$$

It can be shown that P is irreducible and aperiodic. Therefore, there exists a unique stationary probability vector $\bar{\boldsymbol{\pi}}$ satisfying

$$\begin{cases} \bar{\boldsymbol{\pi}} P = \bar{\boldsymbol{\pi}} \\ \sum_i \pi_i = 1. \end{cases} \tag{11}$$

Solving Eq.(11) gives a unique vector $\bar{\boldsymbol{\pi}}$. The average bit error rate, BER, can be computed by summing up the stationary probabilities corresponding to all the states S_k where $\hat{x}_{i-1}$ is different from x_{i-1}. In this case, we have:

$$BER = \pi_1 + \pi_2 + \pi_5 + \pi_6. \tag{12}$$

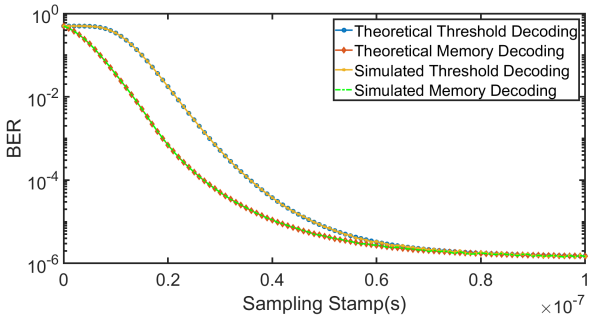

Fig. 3: Classical Threshold Decoding vs. MDA

Fig. 3 shows the comparisons of the normal threshold decoding and memory decoding scheme when the sampling stamp, T_s, ranging from 0 to T for both theoretical and simulated BERs with SNR = 16 dB applied.

IV. Simulations and Discussion

In this section, we show the simulation results for the proposed MDA vs. LMS equalization. The simulation parameters are shown below.

- Data Rate : 100 MHz
- V_{max} : 2 V
- τ_a : 1.77×10^{-9} s
- τ_b : 1.59×10^{-9} s
- Length of training bits : 100 bits

We use training bits to determine τ_a and τ_b at the receiver for MDA and for training LMS equalization algorithm. Fig. 4 shows the BER vs. SNR when AWGN applied with no clock jitter for a number of decoding schemes: classical threshold decoding with a threshold $\frac{V_{max}}{2}$, LMS equalization, and MDA. We simulated for one and two samples per symbol. For one sample per symbol, LMS equalization has almost exactly the same BER with normal threshold decoding, this is because the linear equalization is unable to recover the signals with just one sample per symbol. MDA with one sample per symbol improves the BER a bit compared with the other two schemes. Sampling twice for each symbol can definitely help decoding. The BERs of both classical threshold decoding and LMS equalization reduce from 10^{-5} (one sample/symbol) to about 10^{-7} (two samples/symbol) with SNR of 16 dB. Furthermore, the BER of MDA reduces from 3×10^{-6} (one sample/symbol) to about 3×10^{-9} (two samples/symbol) with the same SNR level. As seen, using MDA results in the lowest bit error rates at the same level SNR. The difference is more pronounced as SNR increases.

For sampling the received signal, the clock jitter is always an issue. Therefore, we also simulated the scenarios when clock jitter is presented. Clock jitter is the deviation from its ideal sampling position. Random jitter caused by thermal noise in an electrical circuit typically follows a normal distribution. Fig. 5 through Fig. 8 simulate

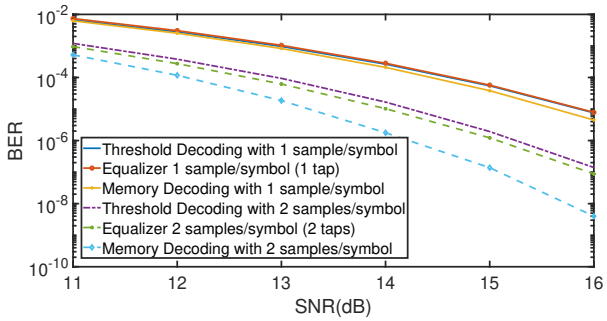

Fig. 4: BER vs. SNR with No Clock Jitter

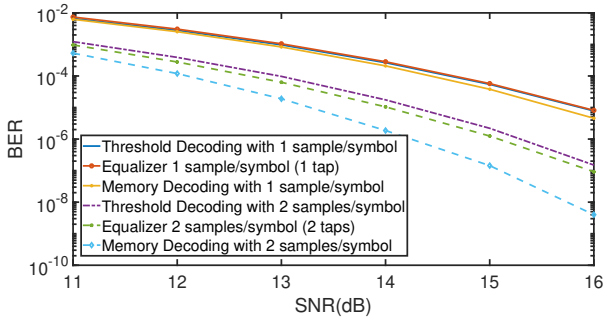

Fig. 5: BER vs. SNR with Clock Jitter $\sim N(0,(1\%T)^2)$

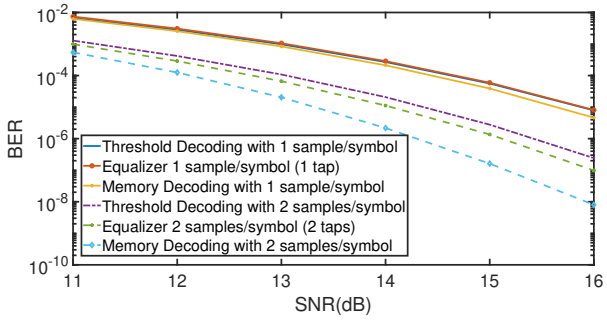

Fig. 6: BER vs. SNR with Clock Jitter $\sim N(0,(2\%T)^2)$

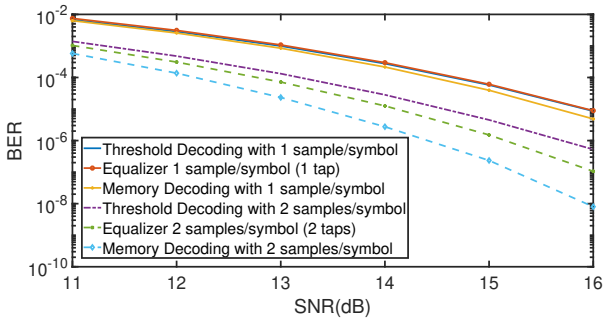

Fig. 7: BER vs. SNR with Clock Jitter $\sim N(0,(3\%T)^2)$

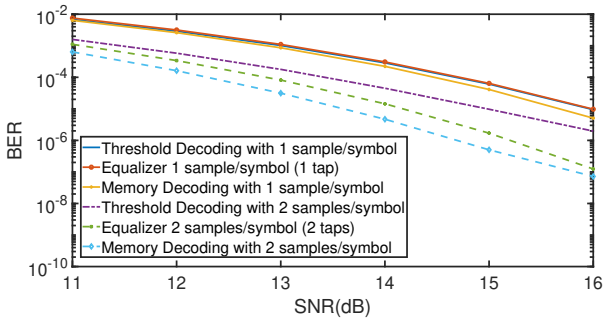

Fig. 8: BER vs. SNR with Clock Jitter $\sim N(0,(4\%T)^2)$

the scenarios when the clock jitter follows a zero mean normal distributions with standard deviations from 1% of T to 4% of T. The simulated results show that MDA still consistently have lower bit error rates than the other schemes when clock jitter increases.

V. Conclusion

In this paper, we utilized a mathematical model to capture the distortion of the output for a given input. Based on the mathematical model, we developed a technique that effectively reduces the bit error rate when On-Off Keying modulation is used. This so called Memory Decoding Algorithm (MDA) is used at a receiver that exploits the distortion model to reduce the bit error rates via maximum likelihood decoding principle. Both theoretical analyses and simulation results show that the proposed technique outperforms the conventional methods such as linear equalization techniques, which require more samples and taps to get lower BER.

References

[1] O. Bouchet, M. El Tabach, M. Wolf, D. O'brien, G. Faulkner, J.W. Walewski, S. Randel, M. Franke, S. Nerreter, K.-D. Langer, J. Grubor and T. Kamalakis, "Hybrid wireless optics (hwo): Building the next generation home network", CNSDSP 2008, pp. 283-287, 2008.

[2] H. Wu, B. Hamzeh and M. Kavehrad, "Achieving carrier class availability of fso link via a complementary rf link", Signals, Systems and Compputers, 2004. Conference Record of the Thirty-Eighth Asilomar Conference, vol. 2, pp. 1483-1487, Nov. 2004.

[3] S. Bloom and W. Hartley, "The last-mile solution: hybrid FSO radio", AirFibber Inc., May. 2002.

[4] I. Kim and E. Korevaar, "Availability of free space optics (fso) and hybrid fso/rf systems", Proc. Optical Wireless Commun. IV, Aug. 2001.

[5] Q. Wang, T. Nguyen and A. Wang, "Channel capacity optimization for an integrated wi-fi and free-space optic communication system(wififo)", 17th ACM MSWIM 2014, ACM, 2014.

[6] Y. Yi, K. Lee, Y. M. Jang, J. Cha, J. Y. Kim and K. Lee, "Indoor LED-Based identification systems using adaptive MMSE equalizer for optical multipath dispersion reduction", International Conference on ICT Convergence Sept. 2011. pp. 95-100 ITCT 2011.

[7] H. Le Minh, Z. Ghassemlooy, A. Burton and P. A. Haigh, "Equalization for organic light emitting diodes in visible light communications", 2011 IEEE GLOBECOM Workshops (GC Wkshps), Dec. 2011.

[8] P. A. Humblet, "Design of optical matched filters", in Proc. IEEE GLOBECOM'91, vol. 2, Dec. 2–5, 1991, pp. 1246–1250.

[9] T. Matsumoto and S. Matsufuji, "Theoretical analysis of BER performance in ASK-SS and M-ary/ASK-SS systems using compact matched filter bank for an optical ZCZ code over

AWGN channels", in Proc. of the 5th International Workshop on Signal Design and its Applications in Communications, pp. 161-164, 2011.
[10] Sun-How Jiang and Feng-Hsiang Lo, "PRML process of multi-level run length-limited modulation recording on optical disk", IEEE Trans. on Magnetism, vol. 41, no. 2, pp. 1070-1072, Feb. 2005.
[11] J. Edwards et al., "A 12.5 Gbps analog timing recovery system for PRML optical receivers", in IEEE RFIC Symp., Jun. 2009
[12] S. Liverman, Q. Wang, Y.J. Chu, A. Borah, S. Wang, A. Natarajan, A. Wang and T. Nguyen, "WiFO: A hybrid communication network based on integrated free-space optical and WiFi femtocells", in Computer Communications, vol. 132, pp. 74-83, November 2018.
[13] S.O. Kasap, "Optoelectronics and Photonics: Principles and Practices", in Prentice Hall, Jan 1, 2001.